

Towards Visual Affordance Learning: A Benchmark for Affordance Segmentation and Recognition

Zeyad Osama Khalifa^a, Syed Afaq Ali Shah^{a,b,*}

^a*Discipline of Information Technology, Murdoch University, Murdoch, WA, Australia*

^b*Center for AI and Machine Learning, Edith Cowan University, Joondalup, WA, Australia*

Both authors have equal contribution and are joint first authors.

Abstract

The physical and textural attributes of objects have been widely studied for recognition, detection and segmentation tasks in computer vision. A number of datasets, such as large scale ImageNet, have been proposed for feature learning using data hungry deep neural networks and for hand-crafted feature extraction. To intelligently interact with objects, robots and intelligent machines need the ability to infer beyond the traditional physical/textural attributes, and understand/learn visual cues, called visual affordances, for affordance recognition, detection and segmentation. To date there is no publicly available large dataset for visual affordance understanding and learning. In this paper, we introduce a large scale multi-view RGBD visual affordance learning dataset, a benchmark of 47210 RGBD images from 37 object categories, annotated with 15 visual affordance categories and 35 cluttered/complex scenes with different objects and multiple affordances. To the best of our knowledge, this is the first ever and the largest multi-view RGBD visual affordance learning dataset. We benchmark the proposed dataset for affordance recognition and segmentation. To achieve this we propose an Affordance Recognition Network a.k.a ARNet. In addition, four state-of-the-art deep learning networks are evaluated for affordance segmentation task. Our experimental results showcase the challenging nature of the dataset and present definite prospects for new and robust affordance learning algorithms. The dataset is available at: <https://sites.google.com/view/afaqshah/dataset>.

Keywords: Dataset, Benchmark, Visual Affordance, Segmentation

1. Introduction

Objects can be represented by various visual features such as shape, color, or physical attributes e.g., material, volume and weight. These attributes of objects are useful for object recognition [1], their segmentation or categorization into different classes, however they do not imply the potential actions that humans or intelligent machines can perform on objects while interacting with them. The ability of humans and machines to understand functional aspects of objects a.k.a

*Corresponding Author

Email address: Afaq.shah@ecu.edu.au (Syed Afaq Ali Shah)

Preprint submitted to -

March 29, 2022

object affordances has been studied for a long time [2, 3]. In contrast to visual and physical attributes that mainly describe the object or its instance, affordance indicates functional interaction of humans with objects.

Object affordance understanding and learning is therefore crucial for intelligent machines such as autonomous robots to interact with objects in static as well as dynamic and complex scenes. Several applications require affordance learning e.g., predicting valid functionality of the objects [4], and recognizing agent's actions in a given environment [5], [6].



Figure 1: Few example images of bowl, flashlight and cereal box from our large scale multi-view visual affordance learning dataset (RGB images and affordance annotations). Affordance labels such as wrap-grasp (green), containment (yellow), grasp (dark red), openable (blue) and rollable (gray) are represented with different colors. Figure best seen in color.

One of the significant modalities for object affordance learning is through visual sensors, which capture visual affordances offered by an object [7]. Visual affordance has been recently explored with computer vision techniques. Luddecke et al., [8] used object parts segmentation to learn affordances. Castellini et al., [9] employed human hand poses during the interaction with objects to define affordances. Sun et al., [10] used object categorization to correctly infer the affordances. To achieve this, they developed an affordance model, which encoded the relationships among visual features, and learned categories and object affordances. A detailed review on the visual affordance understanding techniques and applications can be found in [7].

Deep learning has received unprecedented performance for object recognition, detection and segmentation [11], [12]. In few cases, it has even achieved better performance than humans [13]. The success of deep learning is yet to be seen for visual affordance learning. As pointed in [7], one of the major bottlenecks is the small size of the existing affordance datasets. Deep learning algorithms need large annotated datasets for training and no such dataset is currently available for affordance learning [7], [14]. In addition, the existing datasets are limited to a single view-point of objects [15]. As a result, these datasets are not ideal for deep learning and do not pose significant challenges to modern computer vision techniques.

To encourage research into visual affordance learning, particularly using deep neural networks, a large scale dataset is highly desired. Therefore, in this paper, we propose a large scale multi-view RGBD object affordance learning dataset. Fig. 1 shows sample images from our object affordance dataset. Development of a large scale multi-view dataset is a challenging and subjective task. To handle the subjectivity problem, we take into account the affordance definitions from the existing research on visual affordance learning [7] and select possible affordance labels and interactions one can have with RGBD objects. We define 15 types of affordances over 37 indoor use object categories and 35 complex scenes. In addition, we demonstrate that our dataset also enables benchmarking a wide range of tasks such as affordance recognition and affordance segmentation using deep learning. Three state-of-the-art deep neural networks are evaluated for affordance segmentation task. We also propose an Affordance Recognition Network (ARNet) and evaluate its performance with three popular deep neural networks as the backbone models. It is worth mentioning that affordance learning comes with the key underlying challenges. The same affordance can occur in very diverse scenarios/objects, e.g., a chair can afford sitting and a metal bar at the appropriate height can also afford sitting. In addition, it has one to many correspondences e.g., the same object can afford multiple functionalities. The proposed dataset overcomes these challenges.

The contributions of this paper can be summarised as:

- We introduce a large scale multi-view RGBD affordance learning dataset, consisting of 47210 well-defined affordance information annotations covering 15 affordance classes and 37 object categories. The dataset also provides 35 cluttered scenes with multiple affordance annotations. To the best of our knowledge, this is the first large scale multi-view RGBD dataset for visual affordance learning.
- Our large scale dataset addresses the aforementioned challenges in affordance learning and helps bridge the gap, e.g., in our dataset a coffee mug and pitcher both can afford *liquid containment*, similarly, hand towel and kleenex (tissue) afford *dry* as one of the affordances. In addition, pitcher offers grasp, liquid containment, pourable and wrap-grasp i.e., multiple affordances.
- We propose two affordance learning tasks including affordance recognition and segmenta-

tion to demonstrate the significance of the proposed dataset.

- Our experimental results demonstrate that the proposed dataset is valuable yet challenging for visual affordance learning tasks using deep neural networks.

2. Literature Review

An affordance is the possibility of an action on an object or environment [2]. The idea of affordance learning in general is to identify the purpose, use, and ways to interact with an object, based on information gained from observing the object. It is an implementation of features that are learnt from various object classes, to predict how these objects may be used. Affordance learning is the core requirement in developing intelligent machines. In particular, visual affordance learning is the promising approach due to the diverse and multimodal information captured by the visual sensors. Due to recent advancements in visual sensors and data acquisition technology, a number of object affordance datasets have been developed for affordance recognition, segmentation and detection. In this section, we provide a brief overview of the existing affordance datasets. A summary of these datasets is provided in Table 1.

Affordance Datasets	Year	Modality	Categories	Affordances	Images/frames
AAL [16]	2011	RGBD	6	7	375
CONTACT VMGdB [9]	2011	RGBD	5	1	5200
UMD [17]	2015	RGBD	17	7	30,000
TTU [18]	2015	RGBD	10	-	452
CAD120 [19]	2016	RGBD	35	6	3090
ADE-Affordance [20]	2016	RGBD	7	15	25,000
Extended NYUv2 [21]	2016	RGBD	40	5	1449
HHOI [22]	2016	RGBD	5	5	-
VG Affordance [23]	2016	RGBD	8	1	10360
CRD [24]	2016	RGBD	4	1	1326
IIT-AFF [25]	2017	RGBD	10	9	8835
Binge Watching [26]	2017	RGBD	30	-	11449
CERTH-SOR3D [27]	2017	RGBD	14	13	20800
COQE [28]	2017	RGB	10	1	5000
3D Affordance Net [15]	2021	Point cloud	23	18	56307
Our dataset	2022	RGBD	37	15	47210 + 35 scenes

Table 1: Summary of the existing object affordance datasets (in chronological order) and our multi-view RGBD affordance learning dataset.

Most of the visual affordance datasets consist of RGBD images and videos, except for 3D Affordance Net [15], which contains 3D point cloud data from PartNet [29]. These datasets have been developed to benchmark specific task e.g., visual affordance segmentation and detection (UMD [17], CAD120 [19], ADE-Affordance [20], IIT-AFF [25] and 3D Affordance Net [15]). The other datasets benchmark object grasping and human interaction with objects for visual affordance understanding e.g., Binge Watching [26], HHOI [22], and COQE [28]. These datasets feature 6 to 40 object categories (Table 1), 1 to 15 affordance types (18 for point cloud based 3D

Affordance Net, which is outside the scope of this paper due to a different modality) and 375 to 30k RGBD labelled images. As can be noted, the highest number of object categories can be found in Extended NYUv2 [21], however, this dataset consists of only 5 affordance types. On the other hand, ADE-Affordance [20] features 15 affordance labels, however, it covers only 7 object categories. As also evident from Table 1, the size of existing visual affordance datasets is very small e.g., UMD [17] is the largest RGBD visual affordance dataset, which consists of 30k labelled images. These datasets are not big enough to train and test state-of-the-art deep learning networks. Deep learning based affordance algorithms need large annotated datasets, which are currently unavailable.

To address this challenge, we have created a new large scale multi-view RGBD visual affordance learning dataset, which consists of 37 indoor object categories (sourced from a large scale hierarchical object dataset [30]), 47210 RGBD labelled images, 40 cluttered scenes and 15 affordance types, which are selectively inherited from a summary of existing works. Our dataset can be used to benchmark both visual affordance segmentation and recognition, and can easily be extended for affordance detection. In the following section, we provide details of our affordance learning dataset.

3. Dataset Construction and Annotation

We present a large scale multi-view visual affordance learning dataset for affordance segmentation and recognition. To construct this dataset, raw RGBD images are collected from the Washington RGBD hierarchical multi-view object dataset [30], which covers 51 categories of common indoor objects. The Washington RGBD dataset was captured using a Kinect style 3D camera that records synchronized and aligned 640 x 480 RGB and depth images at 30Hz. Objects were placed on a turntable and video sequences were captured for one whole rotation for each object. For each object, there are 3 video sequences, each recorded with the camera located at a different height relative to the turntable at approximately 30°, 45°, and 60° above the horizon. To avoid significant overlap between frames, we picked every 5th frame for annotation. From the available 51 object categories, we select those (37 object categories only) suitable for affordance learning and removed other objects e.g., fruits (apple, banana, pear etc.) and vegetables (mushroom, onion and potato etc). In addition, we selected 40 complex and cluttered scenes, which contain objects from 37 different categories and annotate these scene with multiple affordances. To ensure that our affordance dataset adds value to the research area we defined a set of affordance categories based on the existing work [7]. In total, 10 annotators were hired and trained for annotations. The average annotation time was around 3 minutes per image and each object category is annotated by two different annotators. All the annotations were verified by two experts.

3.1. Affordance Labels and Annotation Tool

From the list of affordance labels reported in [7], we select those suitable for RGBD objects in [30] and remove the irrelevant ones. In total, we filter out 12 types of affordances including, ‘grasp’, ‘wrap grasp’, ‘containment’, ‘liquid-containment’, ‘openable’, ‘dry’, ‘tip-push’, ‘display’, ‘illumination’, ‘cut’, ‘pourable’, and ‘rollable’. We also introduce three new affordances including ‘absorb’, ‘grip’ and ‘stapling’ for sponge, plier and stapler, respectively. Next, we assign these affordances to each object category according to its functionality and affordances it offers to humans or robots.

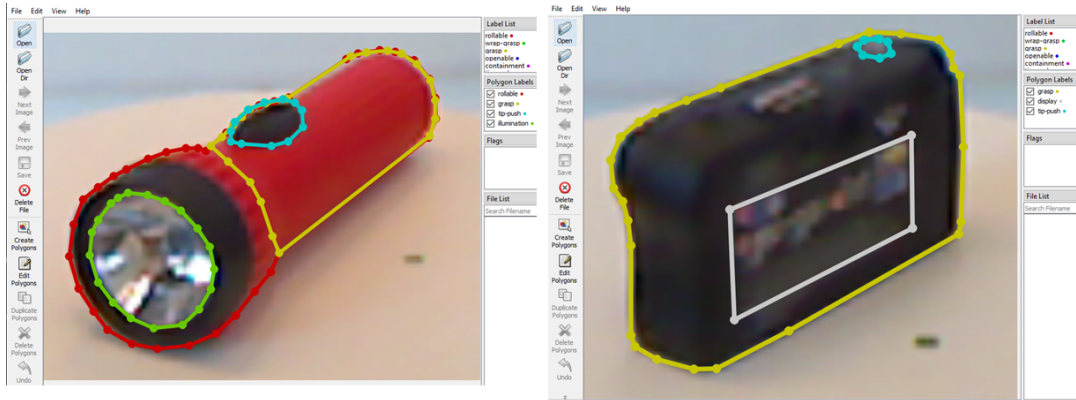


Figure 2: Annotation Tool (LabelMe). Left: Flashlight with four different affordance annotations. Right: Camera with three different affordances.

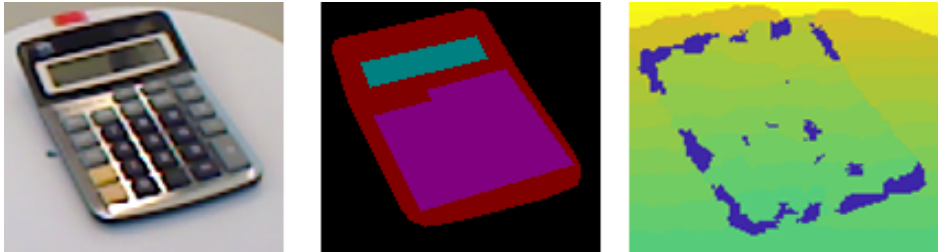


Figure 3: Dataset Annotation. Left: Original RGB image. Center: Annotated image showing affordances such as display, tip-push and grasp. Right: Depth image. It is evident that the depth image is difficult to annotate compared to its RGB counterpart.

For affordance annotation, we used the popular LabelMe graphical tool [31], as shown in Fig. 2. The reason for choosing LabelMe is that it is a free open source tool, and it offers multiple features such as image annotation using polygon, circle, line, rectangle, and points. For our dataset, we used polygons for affordance annotations. We annotated RGB images using LabelMe, as these are visually easy to annotate compared to depth images as shown in Fig 3, and then mapped those annotations on the corresponding depth images as the location of an object and affordance annotations are the same in both types of images.

3.2. Data Statistics

Table 2 reports the statistics of our visual affordance learning dataset. The dataset provides well-defined visual affordance annotations for 37 object categories with at most 4 affordance labels defined for each category. The dataset also contains 51304 affordance annotations from 15 affordance classes. Due to the multi-label nature of the affordance dataset, each object part could be labeled with multiple affordances e.g., pourable and liquid-containment. Fig. 4 and Fig. 5 show affordance annotations for few objects and scenes from our proposed dataset, respectively. Fig. 6 shows the statistics of affordance labels in our dataset.

Objects	Affordances	Num
Ball	rollable, wrap-grasp	1620
Binder	grasp, openable	854
Bowl	containment, wrap-grasp	1260
Calculator	display, grasp, tip-push	1188
Camera	grasp, tip-push	702
Cap	grasp	1034
Cell phone	display, grasp, tip-push	1104
Cereal box	grasp, openable	1188
Coffee mug	liquid-containment, pourable, wrap-grasp	1108
Comb	grasp	950
Dry battery	grasp, rollable	1146
Flashlight	grasp, illumination, rollable, tip-push	1200
Food bag	grasp, openable	1590
Food box	grasp, openable	1624
Food can	openable, rollable, wrap-grasp	1616
Food cup	openable, rollable, wrap-grasp	1624
Food jar	openable, rollable, wrap-grasp	1596
Glue stick	grasp, openable	1570
Hand towel	dry, grasp	1576
Instant noodles	grasp, openable	1596
Keyboard	grasp, tip-push	1192
Kleenex	dry, grasp	1520
Lightbulb	grasp, illumination	992
Marker	grasp, openable	1568
Notebook	grasp, openable	1602
Pitcher	grasp, liquid-containment, pourable, wrap-grasp	680
Plate	containment, grasp	1262
Pliers	grasp, grip	1172
Rubber eraser	grasp	1264
Scissors	cut, grasp	958
Shampoo	openable, wrap-grasp	1444
Soda can	openable, wrap-grasp	1202
Sponge	absorb, grasp	1324
Stapler	stapling, grasp	1186
Toothbrush	grasp	1166
Toothpaste	openable, grasp	1638
Water bottle	openable, wrap-grasp	894

Table 2: Statistics of our affordance learning dataset. First column: Object category. Second column: Affordance classes defined for each object category. Third column: Number of images from each object category.

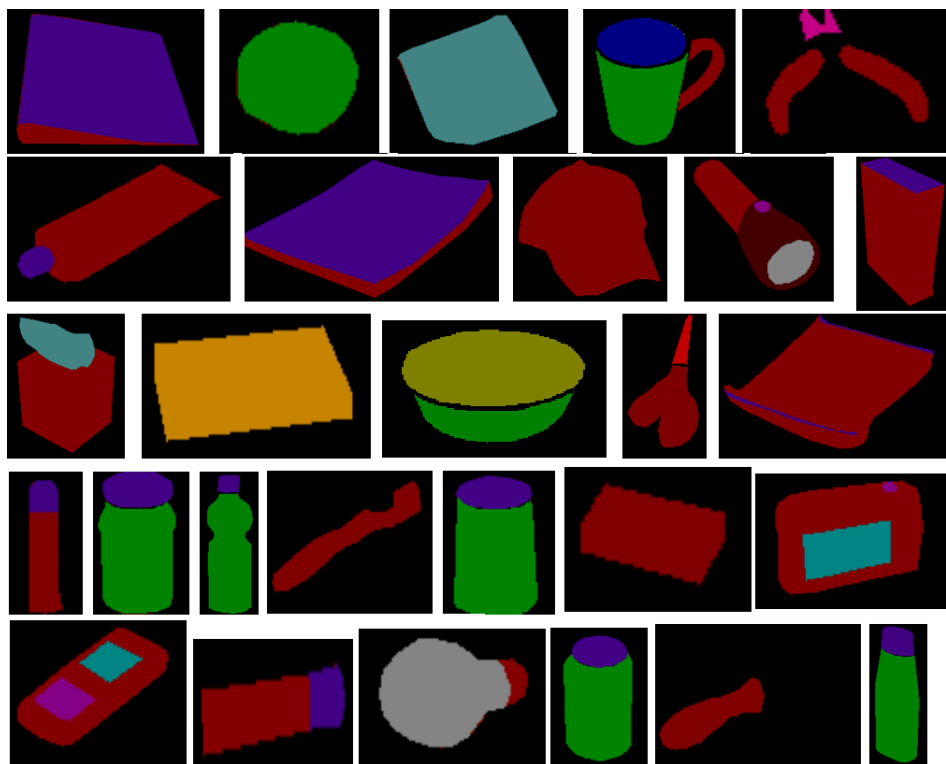
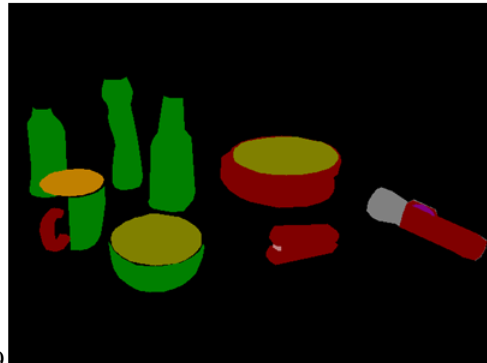
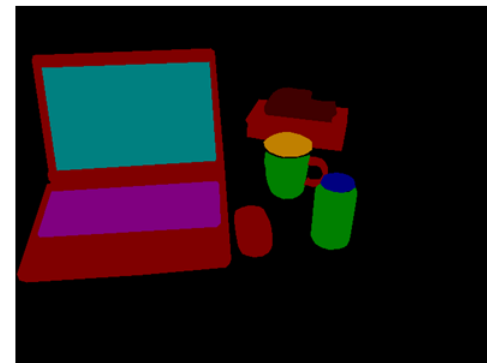
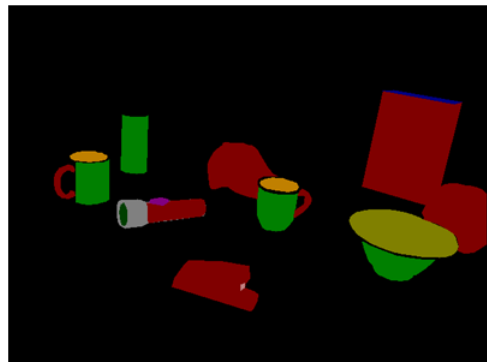
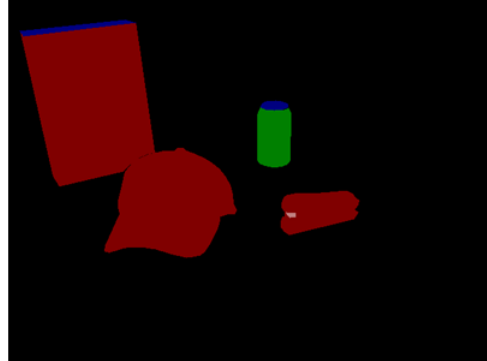


Figure 4: Few example affordance annotations from our dataset. Objects include binder, ball, hand towel, coffee mug, plier, glue stick, food jar, water bottle, shampoo bottle, toothbrush, food can, toothpaste, notebook, cap, flashlight, camera, calculator, glue stick, bulb, tissue box, sponge, bowl, scissors, noodle bag, cereal box, rubber eraser, comb, and soda can. Refer to Table 2 for the affordance labels. Figure best seen in color.



9

Figure 5: Few examples of cluttered scenes, which contain different objects with multiple affordances.

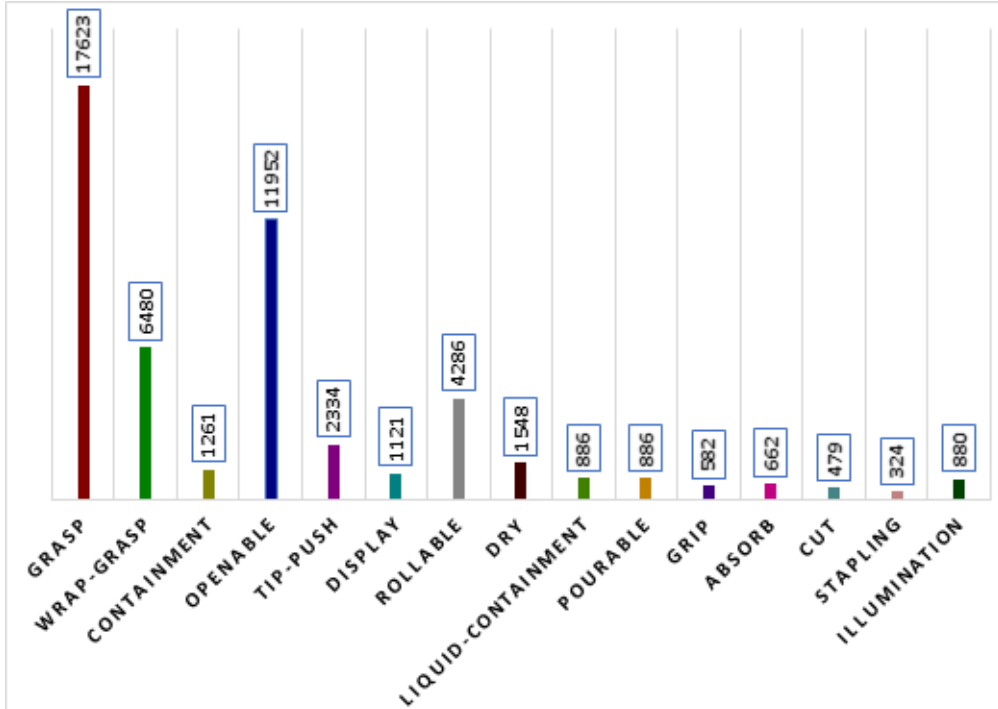


Figure 6: Statistics of affordance labels in our dataset.

4. Benchmarking Results

In this section, we benchmark two major tasks to demonstrate the effectiveness of our visual affordance learning dataset. These tasks include visual affordance segmentation and recognition. The former tackles the pixel-wise labelling of object parts for affordance segmentation and the latter deals with multi-label affordance categorization.

4.1. Visual Affordance Segmentation

Affordance segmentation is a challenging problem. Given an object with not already known affordances, the affordance segmentation task aims to estimate the affordance types supported by the object and predict the pixel-wise probabilistic scores of affordance. For this task, we split the dataset into train and test sets with a ratio of 75% and 25%, respectively. The test set contains totally different shapes of objects, which the deep neural network has not seen during the training process as shown in Fig 7.

In our experiments, we evaluate the following four deep learning architectures, which are described here for completeness.

U-Net [32]: The U-Net consists of an encoder-decoder architecture with skip connections and is build on top of the fully convolutional network. To tackle the information loss problem in the encoder-decoder parts of the U-Net, the network sends information to every up sampling layer in decoder from the corresponding down sampling layer in the encoder. This allows it to capture the required information with low computation cost. Since the initial encoder layers have



Figure 7: Training and test set split. Training and test sets contain unique shapes which makes segmentation task challenging.

more information they bolster the up sampling operation of decoder by providing fine details corresponding to the input images thus improving the segmentation results.

Mobile-Unet [33]: The original mobileNet model is a small model size with faster inference time. This network is ideal to run on mobile phones and resource-constrained devices. In this paper, we use a pre-trained MobileNet as the encoder for the U-Net and integrate it with the U-Net to have an efficient network architecture. There are a few advantages of using MobileNet as the encoder e.g., (i) it has less parameters, due to which it is easy to train, and (ii) a pre-trained MobileNet encoder helps the network to converge much faster.

Pyramid Scene Parsing Network [34]: The Pyramid Scene Parsing Network (PSPNet) is designed to learn global context representation of an object or a given scene. In PSPNet, the input image is fed to the network, which generates a feature map. This feature map is then downsampled to different scales. Next, convolution is applied to the pooled feature maps. All the feature maps generated by the network are then upsampled to a common scale and concatenated together. Finally a convolution layer is used to produce the final segmentation outputs. In this paper, we use two different variants of PSPNet, namely, PSPNet-50 and PSPNet-101.

Co-occurrent Feature Network (CFNet) [35]: CFNet explores the fine-grained representations using co-occurrent features in the given scene and predicts the distribution of co-occurrent features for a given target. To achieve this the network aggregates the probability of the co-occurrent feature within the co-occurrent context.

4.2. Network Training and Evaluation Metrics:

We use pre-trained segmentation models and fine-tune them on our affordance learning dataset. We split the dataset into 75% training images and 25% test images. We use Adam optimizer, categorical cross-entropy loss, and 10 epochs for all our segmentation affordance experiments.

For mobile-Unet, the batch size is set to 64, 16 for U-Net, and 4 for PSPNet-50, PSPNet-101 and CFNet.

For the evaluation of affordance segmentation benchmark, we use the following four evaluation metrics.

Mean Intersection Over Union (mIOU): Mean IOU is a segmentation performance parameter, which measures the ratio of intersection of ground truth and predicted segmentation outputs over their union, and is defined as:

$$\frac{\frac{1}{n_{c0}} * \sum_{\alpha} n_{\alpha\alpha}}{t_{\alpha} + \sum_{\beta} n_{\beta\alpha} - n_{\alpha\alpha}} \quad (1)$$

We calculate IOU of each affordance class and then take their mean. It is an appropriate metric for evaluation in our case as it penalizes both over-segmentation and under-segmentation separately.

Frequency Weighted Intersection Over Union: This is an extension of mean IOU and is defined as follows:

$$\frac{(\sum_{\gamma} t_{\gamma})^{-1} * \sum_{\alpha} t_{\alpha} n_{\alpha\alpha}}{t_{\alpha} + \sum_{\beta} n_{\beta\alpha} - n_{\alpha\alpha}} \quad (2)$$

Since all of our images have background pixels, the chances of class imbalance are very high and the background pixels need to be weighed down compared to affordance classes. Frequency Weighted Intersection Over Union addresses this problem by taking a weighted mean based on the frequency of the class region in the dataset.

Global Accuracy: Global accuracy is the ratio of correctly classified pixels, regardless of class, to the total number of pixels. We use the global accuracy metric as it provides a quick and computationally inexpensive estimate of the percentage of correctly classified pixels.

Mean Accuracy: This metric computes the percentage of correctly identified pixels for each class and it indicates how well each class correctly identifies pixels.

4.3. Affordance Segmentation Results

Table 3 reports segmentation results for our affordance learning dataset. It can be noted that the performance of these four networks is very close as evident from these evaluation metrics. All these models achieve a relatively low mean accuracy and frequency weighted IOU score, which indicates that the affordance estimation is a challenging task for the existing segmentation models. Table 4 reports the accuracy and IOU for each affordance type segmented by the Mobile-Unet. As can be noted, accuracy and IOU for cut are equal to zero. This affordance occurs only 479 in the dataset and only for one object i.e., scissors.

Fig. 8 shows qualitative results for affordance segmentation using Mobile-Unet. As can be noted, the model has correctly predicted pixel-wise affordance labels for different types of objects.

4.4. Multi-label Visual Affordance Recognition

In this section, we discuss our proposed ARNet and report results for visual affordance recognition using the proposed model. The affordance recognition task aims to categorize an image with the relevant set of affordance labels. To achieve this, an image is represented in the form of discriminative features and a classifier is used to predict affordance labels [7]. Affordance recognition is a multi-label problem, as opposed to object recognition, where each image only has one

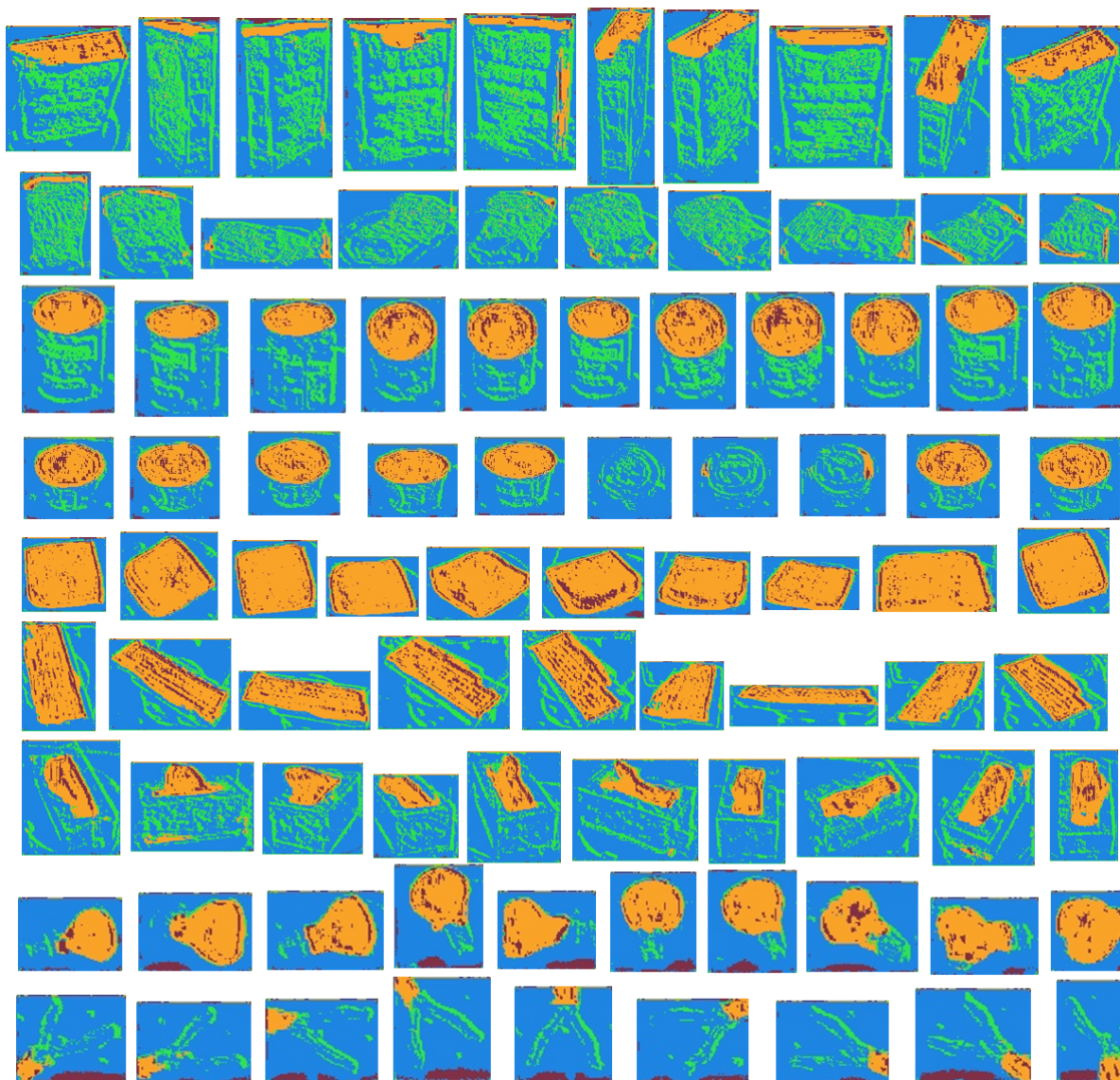


Figure 8: Segmentation results for multi-views of objects using Mobile-Unet. 1st row: Cereal box, 2nd row: Food bag, 3rd row: Food can, 4th row: Food cup, 5th row: Hand towel, 6th row: Keyboard, 7th row: Kleenex box, 8th row: Light bulb, and 9th row: Plier.

Technique	mean IOU	Frequency Weighted IOU	Global Accuracy	Mean Accuracy
U-Net [32]	0.5	0.04	0.3	0.28
Mobile-Unet [33]	0.8	0.05	0.52	0.46
PSPNet-50 [34]	0.9	0.75	0.61	0.5
PSPNet-101 [34]	0.4	0.2	0.3	0.25
CFNet [35]	0.85	0.06	0.6	0.5

Table 3: Visual affordance segmentation results (on a scale of 1). These experimental results demonstrate that our multi-view object affordance dataset is challenging for the state-of-the-art deep learning techniques.

Affordance	Accuracy	IoU
grasp	0.43	0.2
wrap-grasp	0.50	0.4
containment	0.7	0.8
openable	0.34	0.85
tip-push	0.47	0.12
display	0.06	0.14
rollable	0.05	0.6
dry	0.4	0.5
liquid-containment	0.06	0.2
pourable	0.08	0.6
grip	0.4	0.5
absorb	0.67	0.6
cut	0	0
stapling	0.102	0.2
illumination	0.2	0.3

Table 4: Accuracy and IoU for each affordance type.

label. We therefore define and encode labels for each object category, as shown in Table 5, based on the affordance offered by an object. These encoded affordance labels are then used for the supervised training of deep neural networks. Note that the purpose of affordance recognition is not to classify an object, but to predict its affordance e.g., food can and food jar offer the same affordances i.e., wrap-grasp and openable, and can be used in lieu of each other.

4.5. Proposed Affordance Recognition Network (ARNet)

The backbone architecture of our ARNet is inspired by the popular deep learning architectures including VGG-16 [36], ResNet-50 [37] and InceptionV3 [38]. We build on top of these models by adding a dropout layer of 0.5 after the last activation layer and before the last fully connected layer, where the network weights are initialised. The network is then trained with the training data using fine-tuning. We use Adam optimizer, learning rate is set to 0.0001, batch size and epochs are set to 64 and 20, respectively, for all the ARNet configurations.

We ran our experiments 5 folds for all the three models with random selection of training (70%) and test (30%) images. We do not perform any data augmentation and use raw images for the training of these models. Our affordance recognition results are reported in Table 6, which

Objects	Encoded Affordance Labels
Ball	0 1 0 0 0 0 0 0 1 0 0 0 0 0 0
Binder	1 0 1 0 0 0 0 0 0 0 0 0 0 0 0
Bowl	0 1 0 1 0 0 0 0 0 0 0 0 0 0 0
Camera	1 0 0 0 0 1 0 0 0 0 0 0 0 0 0
Cap	1 0 0 0 0 0 0 0 0 0 0 0 0 0 0
Cell phone	1 0 0 0 1 1 0 0 0 0 0 0 0 0 0
Coffee mug	0 1 0 0 0 0 1 1 0 0 0 0 0 0 0
Flashlight	1 0 0 0 0 1 0 0 1 1 0 0 0 0 0
Food bag	1 0 1 0 0 0 0 0 0 0 0 0 0 0 0
Pitcher	1 1 0 0 0 0 1 1 0 0 0 0 0 0 0
Sponge	1 0 0 0 0 0 0 0 0 0 0 0 0 0 1 0
Stapler	1 0 0 0 0 0 0 0 0 0 0 0 0 0 0 1

Table 5: Encoded affordance labels, shown as an example, for few object categories from our dataset. In each row, affordance labels appear in the following order: grasp, w-grasp, openable, containment, display, tip-push, liquid-containment, pourable, rollable, illumination, dry, cut, grip, absorb, stapling. 1 means the affordance type is offered by an object and 0 means the affordance is not available for the object category.

reports average accuracy and the standard deviation. As can be noted our models achieve very good affordance recognition accuracy without any data augmentation, which demonstrate the effectiveness of our large scale multi-view RGBD dataset and its suitability for the training of deep neural networks.

Architecture	RGB (%)	Depth (%)	RGBD (%)
ARNet with VGG-16 [36]	64.96 \pm 5.52	41.6 \pm 0.57	45.625 \pm 3.75
ARNet with ResNet-50 [37]	73.81 \pm 3.98	73.34 \pm 1.57	72.95 \pm 1.69
ARNet with InceptionV3 [38]	81.97 \pm 2.5	80.98 \pm 2.00	80.62 \pm 1.42

Table 6: Visual Affordance Recognition Results report average accuracy and standard deviation. These experimental results demonstrate that our multi-view object affordance dataset is appropriate for the training and testing of deep neural networks without data augmentation.

4.6. Implementation Details

All the deep learning architectures are implemented using TensorFlow and Keras libraries available in Python. The experiments were run on a Windows machine with 64 GB RAM, Core i7-9800X CPU @ 3.80GHz CPU and 12 GB NVIDIA Titan-V GPU.

5. Conclusion

In this paper, we proposed the first ever large scale multi-view RGBD visual affordance learning benchmark, which consists of 47210 RGBD images from 37 object categories, and 40 cluttered scenes annotated, with 15 visual affordance types. Using our dataset, we define two different affordance learning tasks and benchmarked four state-of-the-art deep networks including

U-Net, Mobile-Unet, PSP-50, PSP-101, and CFNet for affordance segmentation. We also propose ARNet architecture for affordance recognition with three different backbone models. Our results demonstrate that the proposed dataset is suitable for the training of deep neural networks for visual affordance learning tasks and without any data augmentation. The results also suggest that more robust techniques are required to perform affordance segmentation on our proposed benchmark. We believe that the proposed dataset will encourage the research community to focus on visual affordance learning research.

Acknowledgments

This research is supported by Edith Cowan University.

References

- [1] S. A. A. Shah, M. Bennamoun, F. Boussaid, Keypoints-based surface representation for 3d modeling and 3d object recognition, *Pattern Recognition* 64 (2017) 29–38.
- [2] J. J. Gibson, *The ecological approach to visual perception: classic edition*, Boston: Houghton Mifflin, 1979.
- [3] S. A. A. Shah, M. Bennamoun, F. Boussaid, A novel 3d vorticity based approach for automatic registration of low resolution range images, *Pattern Recognition* 48 (9) (2015) 2859–2871.
- [4] H. Grabner, J. Gall, L. Van Gool, What makes a chair a chair?, in: *CVPR 2011, IEEE*, 2011, pp. 1529–1536.
- [5] S. Qi, S. Huang, P. Wei, S.-C. Zhu, Predicting human activities using stochastic grammar, in: *Proceedings of the IEEE International Conference on Computer Vision*, 2017, pp. 1164–1172.
- [6] T.-H. Vu, C. Olsson, I. Laptev, A. Oliva, J. Sivic, Predicting actions from static scenes, in: *European Conference on Computer Vision*, Springer, 2014, pp. 421–436.
- [7] M. Hassanin, S. Khan, M. Tahtali, Visual affordance and function understanding: A survey, *ACM Computing Surveys (CSUR)* 54 (3) (2021) 1–35.
- [8] T. Luddecke, F. Worgotter, Learning to segment affordances, in: *Proceedings of the IEEE International Conference on Computer Vision Workshops*, 2017, pp. 769–776.
- [9] C. Castellini, T. Tommasi, N. Noceti, F. Odone, B. Caputo, Using object affordances to improve object recognition, *IEEE transactions on autonomous mental development* 3 (3) (2011) 207–215.
- [10] J. Sun, J. L. Moore, A. Bobick, J. M. Rehg, Learning visual object categories for robot affordance prediction, *The International Journal of Robotics Research* 29 (2-3) (2010) 174–197.
- [11] C.-L. Zhang, Y.-H. Cao, J. Wu, Rethinking the route towards weakly supervised object localization, in: *Proceedings of the IEEE/CVF Conference on Computer Vision and Pattern Recognition*, 2020, pp. 13460–13469.
- [12] Z. Yue, T. Wang, Q. Sun, X.-S. Hua, H. Zhang, Counterfactual zero-shot and open-set visual recognition, in: *Proceedings of the IEEE/CVF Conference on Computer Vision and Pattern Recognition*, 2021, pp. 15404–15414.
- [13] J. X. Chen, The evolution of computing: Alphago, *Computing in Science & Engineering* 18 (4) (2016) 4–7.
- [14] Y. He, Z. Shen, P. Cui, Towards non-iid image classification: A dataset and baselines, *Pattern Recognition* 110 (2021) 107383.
- [15] S. Deng, X. Xu, C. Wu, K. Chen, K. Jia, 3d affordancenet: A benchmark for visual object affordance understanding, in: *Proceedings of the IEEE/CVF Conference on Computer Vision and Pattern Recognition*, 2021, pp. 1778–1787.
- [16] T. Hermans, J. M. Rehg, A. Bobick, Affordance prediction via learned object attributes, in: *IEEE International Conference on Robotics and Automation (ICRA): Workshop on Semantic Perception, Mapping, and Exploration*, Citeseer, 2011, pp. 181–184.
- [17] A. Myers, C. L. Teo, C. Fermüller, Y. Aloimonos, Affordance detection of tool parts from geometric features, in: *2015 IEEE International Conference on Robotics and Automation (ICRA)*, IEEE, 2015, pp. 1374–1381.
- [18] Y. Zhu, Y. Zhao, S. Chun Zhu, Understanding tools: Task-oriented object modeling, learning and recognition, in: *Proceedings of the IEEE Conference on Computer Vision and Pattern Recognition*, 2015, pp. 2855–2864.
- [19] J. Sawatzky, A. Srikantha, J. Gall, Weakly supervised affordance detection, in: *Proceedings of the IEEE Conference on Computer Vision and Pattern Recognition*, 2017, pp. 2795–2804.
- [20] B. Zhou, H. Zhao, X. Puig, T. Xiao, S. Fidler, A. Barriuso, A. Torralba, Semantic understanding of scenes through the ade20k dataset, *International Journal of Computer Vision* 127 (3) (2019) 302–321.
- [21] A. Roy, S. Todorovic, A multi-scale cnn for affordance segmentation in rgb images, in: *European conference on computer vision*, Springer, 2016, pp. 186–201.

- [22] T. Shu, M. S. Ryoo, S.-C. Zhu, Learning social affordance for human-robot interaction, arXiv preprint arXiv:1604.03692 (2016).
- [23] H. O. Song, M. Fritz, D. Goehring, T. Darrell, Learning to detect visual grasp affordance, *IEEE Transactions on Automation Science and Engineering* 13 (2) (2015) 798–809.
- [24] W. Liang, Y. Zhao, Y. Zhu, S.-C. Zhu, What is where: Inferring containment relations from videos., in: *IJCAI*, 2016, pp. 3418–3424.
- [25] A. Nguyen, D. Kanoulas, D. G. Caldwell, N. G. Tsagarakis, Object-based affordances detection with convolutional neural networks and dense conditional random fields, in: *2017 IEEE/RSJ International Conference on Intelligent Robots and Systems (IROS)*, IEEE, 2017, pp. 5908–5915.
- [26] X. Wang, R. Girdhar, A. Gupta, Binge watching: Scaling affordance learning from sitcoms, in: *Proceedings of the IEEE Conference on Computer Vision and Pattern Recognition*, 2017, pp. 2596–2605.
- [27] S. Thermos, G. T. Papadopoulos, P. Daras, G. Potamianos, Deep affordance-grounded sensorimotor object recognition, in: *Proceedings of the IEEE Conference on Computer Vision and Pattern Recognition*, 2017, pp. 6167–6175.
- [28] R. Mottaghi, C. Schenck, D. Fox, A. Farhadi, See the glass half full: Reasoning about liquid containers, their volume and content, in: *Proceedings of the IEEE International Conference on Computer Vision*, 2017, pp. 1871–1880.
- [29] K. Mo, S. Zhu, A. X. Chang, L. Yi, S. Tripathi, L. J. Guibas, H. Su, Partnet: A large-scale benchmark for fine-grained and hierarchical part-level 3d object understanding, in: *Proceedings of the IEEE/CVF Conference on Computer Vision and Pattern Recognition*, 2019, pp. 909–918.
- [30] K. Lai, L. Bo, X. Ren, D. Fox, A large-scale hierarchical multi-view rgb-d object dataset, in: *2011 IEEE international conference on robotics and automation*, IEEE, 2011, pp. 1817–1824.
- [31] B. C. Russell, A. Torralba, K. P. Murphy, W. T. Freeman, Labelme: a database and web-based tool for image annotation, *International journal of computer vision* 77 (1-3) (2008) 157–173.
- [32] O. Ronneberger, P. Fischer, T. Brox, U-net: Convolutional networks for biomedical image segmentation, in: *International Conference on Medical image computing and computer-assisted intervention*, Springer, 2015, pp. 234–241.
- [33] J. Jing, Z. Wang, M. Rättsch, H. Zhang, Mobile-unet: An efficient convolutional neural network for fabric defect detection, *Textile Research Journal* (2020) 0040517520928604.
- [34] H. Zhao, J. Shi, X. Qi, X. Wang, J. Jia, Pyramid scene parsing network, in: *Proceedings of the IEEE conference on computer vision and pattern recognition*, 2017, pp. 2881–2890.
- [35] H. Zhang, H. Zhang, C. Wang, J. Xie, Co-occurrent features in semantic segmentation, in: *Proceedings of the IEEE/CVF Conference on Computer Vision and Pattern Recognition*, 2019, pp. 548–557.
- [36] K. Simonyan, A. Zisserman, Very deep convolutional networks for large-scale image recognition, arXiv preprint arXiv:1409.1556 (2014).
- [37] K. He, X. Zhang, S. Ren, J. Sun, Deep residual learning for image recognition, in: *Proceedings of the IEEE conference on computer vision and pattern recognition*, 2016, pp. 770–778.
- [38] C. Szegedy, W. Liu, Y. Jia, P. Sermanet, S. Reed, D. Anguelov, D. Erhan, V. Vanhoucke, A. Rabinovich, Going deeper with convolutions, in: *Proceedings of the IEEE conference on computer vision and pattern recognition*, 2015, pp. 1–9.